

1 Conformal Prediction quantifies the uncertainty of

2 Species Distribution Models

3 Timothée Poisot — Département de Sciences Biologiques, Université de Montréal, Montréal QC,
4 Canada
5 timothee.poisot@umontreal.ca

6 **Abstract:** Providing accurate estimates of uncertainty is key for the analysis, adoption, and
7 interpretation of species distribution models. In this manuscript, through the analysis of data
8 from an emblematic North American cryptid, I illustrate how Conformal Prediction allows fast
9 and informative uncertainty quantification. I discuss how the conformal predictions can be used
10 to gain more knowledge about the importance of variables in driving presences and absences, and
11 how they help assess the importance of climatic novelty when projecting the models under future
12 climate change scenarios.

13 Introduction

14 The ability to predict where species may be found is a cornerstone of biogeography and
15 macroecology (Elith 2019). Techniques from the field of applied machine learning (ML hereafter)
16 are now routinely used alongside ecological approaches to train generalizable species distribution
17 models (SDMs hereafter) (Beery et al. 2021). SDMs generate a binary response (corresponding to
18 the prediction that the species is likely present/absent under given environmental conditions) or a
19 quantitative score most often as a probability of presence or habitat suitability, indicating how
20 strongly we believe that the species may be present at the location.

21 Proper communication of the uncertainty associated to the prediction of a SDM is important,
22 since we usually seek to apply these models to look both forward and backwards in time
23 (Franklin 2023). This projection if the model to different times is usually called “transfer” (Zurell
24 et al. 2012), whereby a model trained under historical (baseline) conditions is applied to past/
25 future projections of the same predictors. The projection of SDMs can also happen in space
26 (Petitpierre et al. 2016), to predict where species may invade or be naturalized. Even when
27 predictions are not projected, spatial knowledge of the uncertainty is valuable information: it can
28 be used to identify areas where the model predictions are trustworthy. Current checklists on the
29 reproducibility of SDMs emphasize the consequences of data uncertainty (Feng et al. 2019). Yet,
30 predictions also have inherent uncertainty, which is usually not adequately communicated. This
31 can be, for example, because of genuine uncertainty about (or inability to capture through the
32 model) the actual response of the species to combination of predictors (Parker et al. 2024).

33 A common way to capture information about the variability of SDMs is to rely on non-parametric
34 bootstrapping (Valavi et al. 2021), wherein models trained on random subsets of the data are
35 compared to estimate the distribution of the response under incomplete sampling. This approach
36 captures more than one type of variability (Thuiller et al. 2019), and provide valuable information
37 about the range of performances that can be expected from a model. Other methods are built into
38 the predictor itself, as is the case for e.g. BARTs (Carlson 2020), which estimate their own
39 uncertainty. But either situation comes with drawbacks. Bootstrapping requires to train and
40 evaluate the model hundreds of times, and on partial datasets, which is computationally
41 inefficient. Using built-in methods limits one to the classifier for which these methods are
42 available, which prevents for example the use of a new algorithm with the same estimation of
43 uncertainty.

44 In this manuscript, I illustrate how the ML technique of conformal prediction (CP) allows to
45 identify instances (combinations of environmental variables) for which a trained and calibrated
46 model cannot confidently make predictions (Gammerman et al. 1998). A brief introduction to CP
47 is provided in this manuscript, but the topic is covered in more depth by Shafer & Vovk (2007) for
48 the mathematical foundations, by Fontana et al. (2020) for a historical perspective, and by

49 Angelopoulos & Bates (2023) for concrete recommendations. By way of contrast to e.g.
50 bootstrapping, CP does not necessarily involve retraining the same model many times over, but
51 instead wraps the model into an additional prediction step, and returns estimates of credibility
52 based on the distribution of past model predictions compared to ground-truthed data. This is an
53 important difference, as the variability measured through conformal prediction is inherent to the
54 model, and is not a measure of variability coming through the distribution of data (Lei &
55 Wasserman 2013). Conformal prediction provides what is essentially (for classification problems)
56 a confidence interval around the presence or absence of a species in a given location. This is a
57 particularly important feature, in that CP achieves this in a way that creates several analogues
58 between ML prediction and fundamental concepts in frequentist statistics (Neyman 1937).

59 One of the reasons why CP is particularly promising for uncertainty quantification in SDMs is
60 that it is a distribution-free method: it requires neither assumptions about the model nor prior
61 knowledge of the outcome distribution to provide confidence intervals that are as small as
62 possible while being *guaranteed* to contain the true value under a set risk level (Vovk et al. 2018).
63 This is particularly important when transferring a SDM to novel environments (Zurell et al. 2012),
64 where we expect covariate shift (the joint distributions of predictors are different when training
65 and predicting), a prediction context that CP is robust to (Fannjiang et al. 2022, Tibshirani et al.
66 2019).

67 Using occurrence data about an emblematic North American cryptid, I provide a template for the
68 adoption of CP as a natural way to quantify uncertainty of species distribution models. In
69 particular, I show how predictions under CP (i) identify areas where the species range is
70 uncertain, (ii) estimate uncertainty differently from bootstrapping methods, (iii) can be explained
71 using Shapley values analysis, and (iv) quantify the accumulated uncertainty when transferring
72 the SDM to future conditions. I conclude by highlighting ways in which using CP can both
73 simplify the process of training SDMs, and provide information that make their discussion and
74 analysis more informative.

75 **Methods**

76 *Data*

77 **Occurrence data**

78 The occurrence data used in this article are geo-referenced observations of the Sasquatch (Lozier
79 et al. 2009). Although these observations are likely to be mis-categorized American black bears
80 (Foxon 2024), they nevertheless share many features of the data that are used to train SDMs: high
81 auto-correlation, uneven sampling effort, and clear association with several bioclimatic variables
82 that is robust enough to train a predictive model. The recorded locations, as well as background
83 points, are presented in Figure 1.

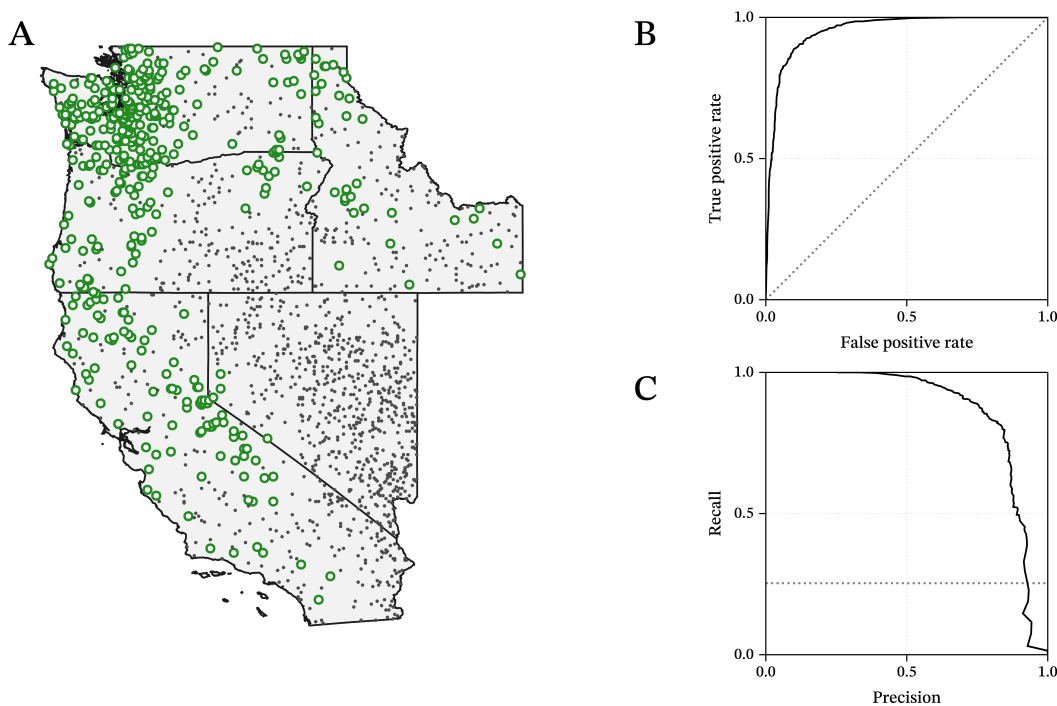
84 **Pseudo-absences generation**

85 The dataset of observations is composed only of presences. In order to establish a baseline of
86 absences to train a binary classifier, there is a need to generate a number of pseudo-absences,
87 which simulates locations at which the species, if not absent, has not been observed. In order to
88 do so, the presence data were first spatially thinned to be limited to one for each cell, at a 5.0
89 minutes of arc resolution. Cells that had no observation were potential candidates for a pseudo-
90 absence, and were further selected by drawing a number of them, without replacement, where
91 the probability of inclusion in the sample was proportional to h_{\min}^{-1} , where h_{\min} is the Haversine
92 (great arc) distance to the nearest cell with an observation, measured in kilometers. In other
93 words, cells that were close to an observation were unlikely to be included, and cells that were
94 further away were more likely to be so. To avoid sampling pseudo-absences too close to presences,
95 the pixels less than 10 kilometers away from known observations were excluded from the
96 background data.

97 The number of pseudo-absences was arbitrarily set to two times the number of presences.
98 Although Barbet-Massin et al. (2012) recommend to use the same number of presences and
99 pseudo-absences for classifiers, using an imbalanced dataset is not a problem: stratified k-folds
100 cross-validation is perfectly able to handle the moderate class imbalance we introduce
101 (Szeghalmy & Fazekas 2023), and the model performance (as will be established in a later section)
102 is sufficient. Moreover, most real-world applications of classification will have to deal with
103 problems with class imbalance (this is particularly likely to be true of SDM application from
104 sampling data, where presences may be the minority of outcomes); it is therefore important to
105 ensure that we do not establish a testing scenario that is too optimistic about the prevalence of
106 presences. In all cases, class imbalances is a feature of data that must be dealt with in order to get
107 the more predictive models (Benkendorf et al. 2023).

108 **Bioclimatic data**

109 The model was trained, validated, and applied on the 19 WorldClim2 BIOCLIM variables (Fick &
110 Hijmans 2017), at a spatial resolution of 2.5 minutes of arc. Preliminary analyses using 0.5, 2.5, 5,



111 Figure 1: Overview of the occurrence data (green circles) and the pseudo-absences (grey points) for the
112 states of, clockwise from the bottom, California, Oregon, Washington, Idaho, and Nevada (A). The
113 underlying predictor data are at a resolution of 2.5 minutes of arc, and represented in the World Geodetic
114 System 1984 CRS (EPSG 4326). The panels on the right column show the ROC curve (B) and PR curve (C),
115 with the random classifier indicated by a dotted line. The area under the ROC curve is $\approx 96\%$.

116 and 10 minutes of arc show that the qualitative results presented hold. For the projection of the
117 model under climate change, I only report the future data under the SSP370 scenario (“business
118 as usual”), for the MRI ESM2-0 GCM, over the period 2081-2100.

119 The climatic novelty of the baseline *v.* future data is estimated through the Euclidean distance
120 (Fitzpatrick et al. 2018), specifically by assigning as a novelty score for each pixel in the future the
121 distance to its closest baseline analogue. This novelty is measured on de-meanned predictors with
122 unit variance.

123 *Species distribution model*

124 All analyses are conducted using the `SpeciesDistributionToolkit` package (Poisot et al. 2025) for
125 *Julia* 1.11.

126 **Model structure**

127 The model used here is a logistic regression, with interactions terms up to a maximum degree of
128 two (preliminary analyses with random forests, naive Bayes classifiers, and rotation forests gave
129 similar results). When trained on a vector of features \mathbf{x}_i (with null means and unit variances), the
130 model will return a probability p_+ , which correspond to the probability of these environmental
131 conditions being associated to the presenceof the species. This probability is turned into a
132 presence/absence decision by comparing it to a threshold, as explained in a later section. Because
133 this logistic regression is a deterministic classifier, the prediction $p_i +$ statisfies $0 \leq p_i + \leq 1$, and
134 we use $p_- = 1 - p_+$ as the probability that the species is absent from the location.

135 **Tuning**

136 We tune this model by (i) iteratively forward selecting the best set of predictor variables, and (ii)
137 optimizing the threshold τ above which a site with a probability for the positive class p_+ is
138 considered to be positive (turning the prediction of presence into $p_+ \geq \tau$). In both cases, the
139 cross-validation strategy is the same: the dataset is split in 10 random folds, 9 of which are used
140 for training and one for validation. All folds are used for evaluation, providing exhaustive cross-
141 validation. The folds are stratified so that the relative number of present cases in the training set

142 is similar to that of the entire dataset. The performance on each set, for the purpose of defining
143 the set of variables to include of the threshold to use, is measured as the average of the Matthews
144 Correlation Coefficient (MCC) across each of the ten folds. The MCC is the most accurate
145 representation of a binary classifier performance (Chicco & Jurman 2023), and avoids the pitfalls
146 of several other validation measures.

147 For all steps of model training and validation, the identity of instances composing the different
148 folds remains fixed. This ensure that the changes in MCC are only due to the addition of the
149 variable, and not to the random sampling of a training/validation set with different properties.
150 Although some authors encourage the use of spatially-stratified cross-validation (Soley-Guardia
151 et al. 2024), this is not a desirable strategy for this use-case. The area in which the predictions will
152 be made is entirely delimited by the bounding box of observed presences, and there is therefore
153 no risk of covariate shift when shifting from validation to prediction (outside of the situation of
154 temporal transfer of the SDM).

155 The predictors included in the model have been decided through the use of forward selection.
156 This is an important step in order to perform dimensionality reduction (which generally increases
157 the predictive accuracy), but also to ensure that the set of retained variables is reduced enough
158 that it can be interpreted. Variables were retained as part of the final set of predictors if adding
159 them increased the MCC for the model once retrained with this new variable.

160 One of the most efficient ways to increase the performance of binary classifiers is to change the
161 decision rule leading to a positive (here, presence) prediction, so that presences are assigned
162 when $p_+ \geq \tau$ – a process known as moving threshold classification (Liu et al. 2013, 2016). The
163 value of τ is an hyper-parameter of the model, which is chosen to maximize the value of a
164 measure of model performance (here the MCC) when evaluated over many different values. In
165 this instance, we optimized the value of τ by picking the value out of 200 linearly spaced value
166 between the smallest and largest prediction made on the training set. The value of τ that
167 maximizes the MCC during cross-validation was selected as the optimal threshold for the
168 classifier. Note that even though our decision rule for the presence of the species is $p_+ \geq \tau$, we
169 will keep the information about p_- as is required for conformal prediction.

170 **Bootstrap variability**

171 Bagging (bootstrap aggregating) is often used as a measure of uncertainty to the underlying data
172 when training SDMs (Beale & Lennon 2012). When performing bagging, the model is trained on
173 samples drawn with replacement from the training set (which leaves out approx. 37% of the
174 dataset). Models are then evaluated on samples that were not used as part of their training,
175 usually using cross-validation (Bylander 2002) or measures of the out-of-bag error (Janitz &
176 Hornung 2018). Although ensemble models *can* result in a better predictive performance
177 compared to single models (Drake 2014), this is not a guarantee (and depends on the structure of
178 the bias/variance trade-off for the specific model and its training set). The many models trained
179 on the bagging dataset form an homogeneous ensemble, which is to say a set of models that share
180 the same algorithm and hyper-parameters, and only make different predictions as the result of
181 having been trained on different subsets of the full training set.

182 Measures of whether the different models composing the homogeneous ensemble agree can
183 provide a measure of the effect of data and parameter uncertainty (Petropoulos et al. 2018), or
184 what Davies et al. (2023) termed the “SDM uncertainty”. The best model identified after
185 thresholding was evaluated on a hundred bootstrap samples, yielding an homogeneous ensemble
186 model from which we estimate bootstrap variability (Chen et al. 2019). Because the model is kept
187 constant in this analysis, the measure of variability we will derive from the ensemble model is an
188 estimate of how sensitive the estimation of the model parameters is to small perturbations
189 (specifically: spatially homogeneous under-sampling) to the training data.

190 **An introduction to conformal prediction**

191 Conformal prediction differs from regular prediction in that, rather than a single point prediction,
192 it returns sets corresponding to the ensemble of *credible* outcomes given an input x representing
193 environmental conditions at which we seek to make the prediction. Given the observed quantiles
194 of the model output on validation data, these sets are obtained through a simple calibration step.

195 Therefore, CP requires an already trained model, and is agnostic to the process through which
196 this model is trained. In this section, I highlight two important features of CP: the notion of
197 *credible sets* (and how they are obtained), and the notion of *coverage*, which is a measure of
198 tolerance to error.

199 *Understanding conformal predictions*

200 By contrast to the non-conformal SDM, the conformal classifier returns, for an input of
201 environmental predictors \mathbf{x} , a set C containing the “credible outcomes” for this prediction. This
202 set is termed the *credible set*, and under a binary classification task (the species is either present or
203 absent), there are four possible combinations for the content of credible sets: $C = \{+\}$, $C = \{-\}$,
204 $C = \{+,-\}$, and $C = \emptyset$.

205 The first two cases are simple: if the credible set contains a single output, the model can
206 confidently make a prediction that excludes the other class. In the case of $C = \{+\}$, for example,
207 the point prediction for the presence score p_+ is high enough that the outcome of absence can be
208 ruled out given the known predictions on training examples. In some cases, the credible set may
209 contain both classes, as in $C = \{+,-\}$. Although they may not be *equally likely* (there is no
210 guarantee that $p_+ \approx p_-$), the scores are close enough to not confidently exclude one of the
211 outcomes from the model prediction. In the specific cases of SDMs, these correspond to areas of
212 true uncertainty, where the known training examples credibly support both the presence or
213 absence of the species. The final situation, $C = \emptyset$, corresponds to pathological cases where
214 *neither* outcome can be credibly supported. Given the training data (and the distribution of
215 presences and absences), the model is not able to make a prediction for this input. The increased
216 frequency of such predictions is most likely a strong sign that the risk level is too high (the
217 confidence interval is too broad) for the training data given to the conformal model.

218 These situations correspond to four different outcomes in terms of the SDM certainty about the
219 distribution of the species. The most intuitive situation is $C = \{+\}$ or $C = \{-\}$, in which case the
220 conformal model predicts that the absence (resp. presence) of the species is *not* a credible
221 outcome for the environmental conditions given as an input. Throughout this manuscript, I will

222 refer to these predictions as “sure presences” and “sure absences”, as they convey the information
223 that there is no reason to expect that the prediction is uncertain. The second situation, $C = \{+, -\}$,
224 corresponds to inputs for which the presence and the absence of the species are credible, and I
225 will refer to them as “unsure”. The rare cases where $C = \emptyset$ will be “undetermined” predictions.

226 *Obtaining conformal predictions*

227 There are several ways to decide whether a point prediction from the model results in which
228 credible set. A core assumption of CP is that the data used for training should be exchangeable, or
229 in other words, their joint probability distribution should be (close to) invariant under finite
230 permutations (Aldous 1985). This will almost never be the case for data with a spatial structure;
231 nevertheless, this does not rule out the use of CP for species distribution modeling, as Oliveira et
232 al. (2024) show that CP is acceptably robust to lack of exchangeability.
233 The central idea of CP is to associate a conformal score to a point prediction. This can be achieved
234 by applying the softmax function to the values for p_+ and p_- , giving

$$s_+ = \frac{\exp p_+}{\exp p_+ + \exp(1 - p_+)}, s_- = \frac{\exp(1 - p_+)}{\exp p_+ + \exp(1 - p_+)} \quad (1)$$

235 The conformal score associated to a prediction is $1 - s_\cdot$, where \cdot is the prediction (+ or -) made
236 by the model. We call the distribution of conformal scores \mathcal{S} . Note that this can be done without
237 using the softmax function, but it is included here as it is best practice for classification.
238 The next step is to identify a critical value \hat{q} above which a conformal score indicates that the
239 prediction it describes is credible. This critical value is picked by examining the empirical
240 quantile distribution of the conformal scores calculated over n training examples, and an
241 acceptable level of risk α (explained in depth in the next sub-section), and specifically by
242 identifying the q_i -th quantile, where

$$q_i = \frac{[(n + 1)(1 - \alpha)]}{n} \quad (2)$$

243 The corresponding value of S below which a proportion q_i of values lies is \hat{q} . In other, more
244 intuitive words, the value q_i indicates what proportion of wrong classification events we must
245 accept before we have accumulated enough evidence to be confident about a prediction. When
246 performing the prediction, we calculate the score of a new prediction according to Equation 1.
247 For every possible class x , if $s_x \geq (1 - \hat{q})$, this class is retained as part of the credible set.
248 The value of \hat{q} can be obtained either through using a holdout set for training (Split Conformal
249 Prediction), by retraining the model in a way akin to Leave-One-Out cross-validation (Full
250 Conformal Prediction), through the use of quantile regression (Romano et al. 2019), or through
251 taking the median of several estimates of \hat{q} after cross-validation (Vovk et al. 2018). In this
252 manuscript, I employ the later method, as it provides a rapid and statistically acceptable estimate
253 of \hat{q} , without requiring too much computing time.
254 To summarize, the output of the conformal classifier is, in a sense, a point estimate of the credible
255 outcomes of a model, using the value estimated for p_+ as well as knowledge about which of these
256 were associated to the correct label in the training data. A location is defined as included in the
257 range if the positive outcome is included within the credible set returned by the conformal
258 classifier, and as excluded from the range when it is not. Because the conformal classifier can
259 identify that both outcomes are credible based on the training data (while giving them different
260 weights), predictions in which both the positive and negative outcomes are included in the
261 credible set can be seen as “uncertain” at this given risk level.
262 How frequently a specific prediction is uncertain is termed the inefficiency of the classifier, which
263 is defined as the average cardinality of all credible sets. The inefficiency is bounded upwards by
264 the number of classes (two for binary classification); when the inefficiency is ≈ 1 , the conformal
265 classifier behaves (essentially) like deterministic classifier, by returning a single class for each
266 instance. An inefficiency close to unity is not desirable: smaller sets can hide our actual
267 uncertainty (Sadinle et al. 2018). Because the conformal models wraps the logistic regression
268 model, we can further divide the “unsure” predictions as a function of whether they would be
269 within the range as predicted by the SDM, which I will call “unsure presences”; the other unsure
270 predictions are referred to as “unsure absences”.

271 *The coverage level*

272 CP allows users to set a desired error rate, α , which appeared in Equation 2. Intuitively, what CP
273 does, is inform the user on whether the credible set contains the true value with probability $1 - \alpha$,
274 which allows to directly interpret this value as a true confidence interval. This error rate is usually
275 referred to as the *marginal coverage*, in that it captures the probability of success marginalized
276 over the known validation points. Because the estimate of uncertainty involves the original
277 model, it is important to apply CP on a model with adequate performance.

278 Chaning the risk level α leads to different estimates of how commonly multiple classes will be
279 accepted as a credible outcome. Using a low level of risk ($\alpha \approx 0$) yields usually leads to all
280 outcomes being credible ($\hat{q} \approx 1$), at the cost of a very high uncertainty. When values of α get too
281 large ($\hat{q} \approx 0$), no class can be confidently predicted, and the model will eventually always return
282 $C = \emptyset$. Although this later situation is more difficult to make sense of intuitively, a value of
283 inefficiency that gets smaller than unity should be interpreted as a model that accumulates more
284 uncertainty (at a given risk level) than the data can support (Romano et al. 2020). Conformal
285 prediction can therefore inform us on the acceptable risk levels we can operate under given a
286 trained predictive model.

287 In the rest of this analysis, I will set $\alpha = 0.05$. As noted by Angelopoulos & Bates (2023), this
288 corresponds to estimating whether a specific prediction falls within, or outside of, the 95%
289 confidence interval across all predictions, which is a convenient callback to frequentist statistics'
290 usual risk tolerance. Recall that the CP credible sets are estimated based on the model output, and
291 therefore even when aiming for full coverage, there may be non-ambiguous combinations of
292 environmental predictors.

Measure	Validation	Training	Ensemble
MCC	0.75	0.76	0.76
NPV	0.93	0.93	0.94
PPV	0.82	0.83	0.82
κ	0.75	0.76	0.76
TSS	0.74	0.75	0.76
Accuracy	0.91	0.91	0.91

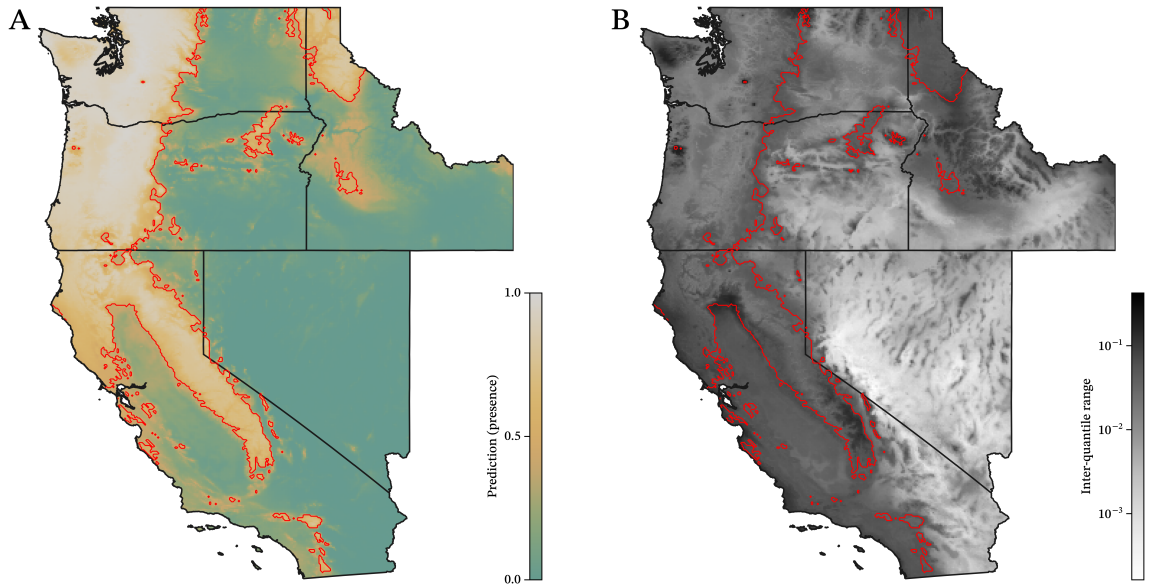
Table 1: Overview of measures of model performance for the validation and training sets of the SDM, as well as the same measures for the ensemble model (measured on the out-of-bag models only). The values of κ and the true-skill statistic are generally comparable to the MCC, but are included as they are commonly reported in the SDM litterature (Allouche et al. 2006). The high values of the negative and positive predictive values indicate that the model is suitable to detect both presences and absences.

Results

Performance of the baseline model

In panels B and C of Figure 1, we report the ROC and PR curves for the model. As evidenced by both these diagnostic tools, the model achieves a very high predictive accuracy. In Table 1, we report additional measures of performance for the training and validation set of the model (so as to ensure that the model is not performing better on training data), as well as a measure of the performance of the ensemble, to show that it can make valid predictions in addition to quantifying variability. These results confirm that the model is able to identify areas that are suitable to the species, and can be used for CP.

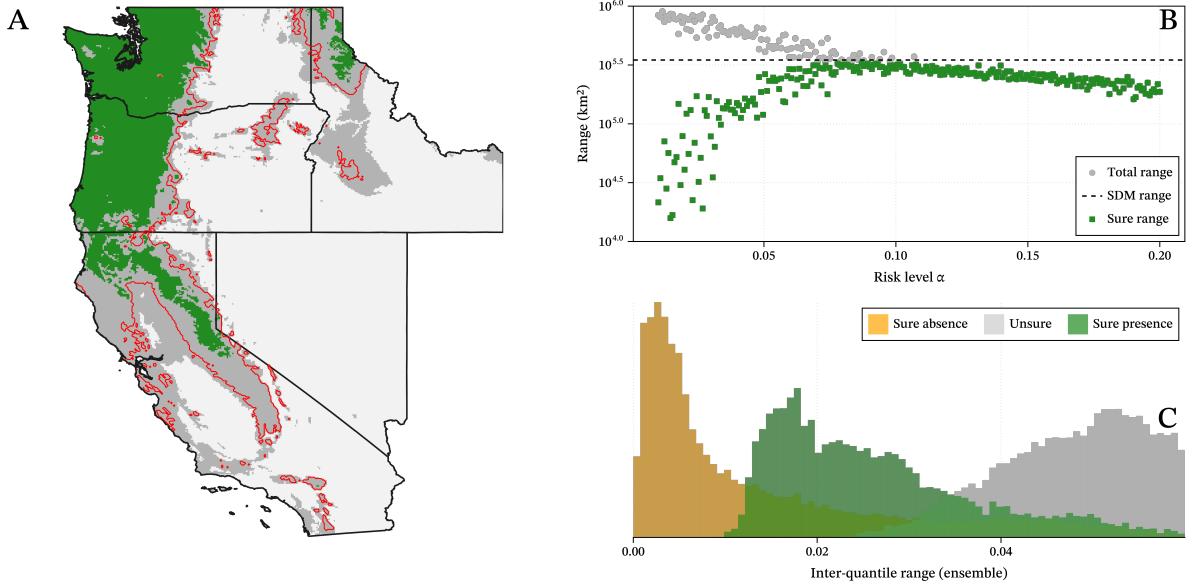
Before applying CP, it is useful to examine the output of the SDM in space. The predictions of the model for the entire region are given in Figure 2, alongside information about the model variability. Areas of lowest variability (according to the IQR based on non-parametric bootstrap results from the ensemble) seem to be associated with the absence of the species, with the variability mostly increasing within the predicted range.



319 Figure 2: Overview of the probability p_+ returned by the model (A), and the inter-quantile range of the
 320 non-parametric bootstrap model predictions (B). The range, i.e. the limit of cells for which $p_+ \geq \tau$, is
 321 indicated by a solid red line; I maintain this convention for all subsequent figures. Note that the scale of the
 322 variability is logarithmic, as the model shows good performance and therefore has low variability overall.

323 *Conformal prediction of the species range*

324 Before discussing the spatial output of running the conformal model, it is worth considering why
 325 the thresholding step as visualized in Figure 2 is not really providing us with a set of certain
 326 presences and absences. When optimizing the threshold τ above which a prediction p_+ from the
 327 non-conformal model is determined to be a presence, we inherently establish a sort of certain
 328 presences and certain absences, specifically by ignoring the possibility that there can be uncertain
 329 predictions. Indeed, the space covered by positive predictions is usually interpreted as the
 330 (potential) distribution of the species. But this prediction conveys a false sense of certainty, that
 331 has to do with the very nature of the threshold we optimize. By definition, the threshold is the
 332 value that finds the best balance between the false/true positive/negative cases on the validation
 333 data; this is in fact why the optimal threshold is the point closest to the corners of the ROC and
 334 PR curves indicating a perfect classifier (Balayla 2020). When a prediction p_+ gets closer to the
 335 threshold, a small perturbation to the environmental conditions locally could bring it on the other
 336 side of the threshold, and therefore flip the predicted class using the non-conformal classifier.
 337 Around the threshold is where we expect uncertainty to be the greatest.



338 Figure 3: Overview of areas where the presence of the species is certain according to the CP model under a
 339 risk level $\alpha = 0.05$ (A). The certain areas are in dark green, and the uncertain areas, wherein both presence
 340 and absence are credible, are in dark grey. (B) Surface covered by the sure absence and total range
 341 (including the superficy of the unsure area) for different risk levels. Note that for $\alpha \approx 0.1$, the total
 342 predicted range starts being lower than the range predicted by the SDM, and the uncertain range collapses.
 343 (C) Distribution of variability from Figure 2B by type of CP model outcome.

344 To bring these considerations into a spatial context: we expect the areas where the score for the
 345 present class are closer to the threshold (the limits of the predicted range of the species) to be the
 346 most uncertain. Importantly, this is true *both* for areas that are inside the range (for which p_+ is
 347 just above the threshold) and for areas that are outside of it (for which p_+ is just below the
 348 threshold). CP is perfectly suited to solving this issue, by identifying the areas where one class is
 349 predicted, but the other class is also credible. In this section, we will project the areas with
 350 uncertain predictions, and compare the uncertainty quantified by the conformal model to the
 351 uncertainty derived from the ensemble model.

352 In Figure 3, we show that this prediction indeed stands: the range as predicted by the SDM
 353 (fig. 3A) falls within the range of unsure predictions. We also see that lowering the risk level α
 354 leads to a contraction of the area (in km²) considered to be credibly associated to only the
 355 presence of the species ($C = \{+\}$), while the range that is ambiguous ($C = \{+, -\}$) increases
 356 (Figure 3B). As far as ecologists are concerned, the areas in which the credible set only has a score
 357 for the absence of the species are the easiest to make sense of: they correspond to regions where
 358 the model is certain (under the specified risk level) that the species is absent. All other areas

359 (assuming that there are no predictions for which the credible set is empty, which I discuss in the
360 next section) are *potentially* part of the range of the species: some certainly, some uncertainly.
361 Depending on the purpose for which the SDM is produced, the uncertain areas can be treated
362 differently. As Prescott et al. (2025) argue, when dealing with invasive species, it may be more
363 reasonable to interpret SDMs by erring on the side of caution, which here would mean
364 considering that unsure presence area should be considered part of the species's range. On the
365 other hand, when SDMs are meant to guide conservation actions that are costly or should be
366 focused on areas of high certainty of suitability for the target species (Pěknicová & Berchová-
367 Bímová 2016), it may make sense to ignore the unsure presences.

368 *Relationship between variability and uncertainty*

369 Note that the relationship between the certainty associated to CP, and the variability under the
370 ensemble model presented in Figure 2B is nuanced: in fig. 3C, it appears that although areas
371 identified as unsure using CP tend to have higher variability, there is considerable overlap
372 between the categories. Intriguingly, the overlap between areas that are uncertain according to
373 the conformal classifier, and areas that are uncertain according to the bootstrap model, is
374 imperfect. There are a number of points classified as sure presences for which the IQR is very
375 high, **i.e.** points whose certainty is not affected by undersampling the training data. Notably, the
376 results in fig. 3C show that it is not possible to find a cutoff in the measure of bootstrap variability
377 that would identify areas of model uncertainty. This suggests that the classification of predictions
378 as certain/uncertain according to the conformal prediction is in part reflecting genuine
379 uncertainty in the underlying data, but also contributing novel information about the fact that
380 some instances are more difficult to call.

381 These results can be better understood by contrasting what “uncertain” means in the context of
382 CP, and how it differs from the uncertainty in the ensemble model. The uncertainty derived from
383 the ensemble model represents whether many models trained on small perturbations of the full
384 training dataset would agree on a specific prediction task, represented by an array of
385 environmental predictors. Therefore, the uncertainty from the ensemble originates in the

386 estimation of the parameters, and its sensitivity to being able to access the full information within
387 the training data. Uncertainty in the conformal classifier is coming from comparing the
388 prediction to all other predictions under an estimation of the distributions for the conditions
389 leading to the prediction of the presence (or absence) outcome. Therefore, the uncertainty from
390 the conformal predictors accounts for all the predictions the model can make, and accounts for
391 the variability *across* predictions within a fully known dataset.

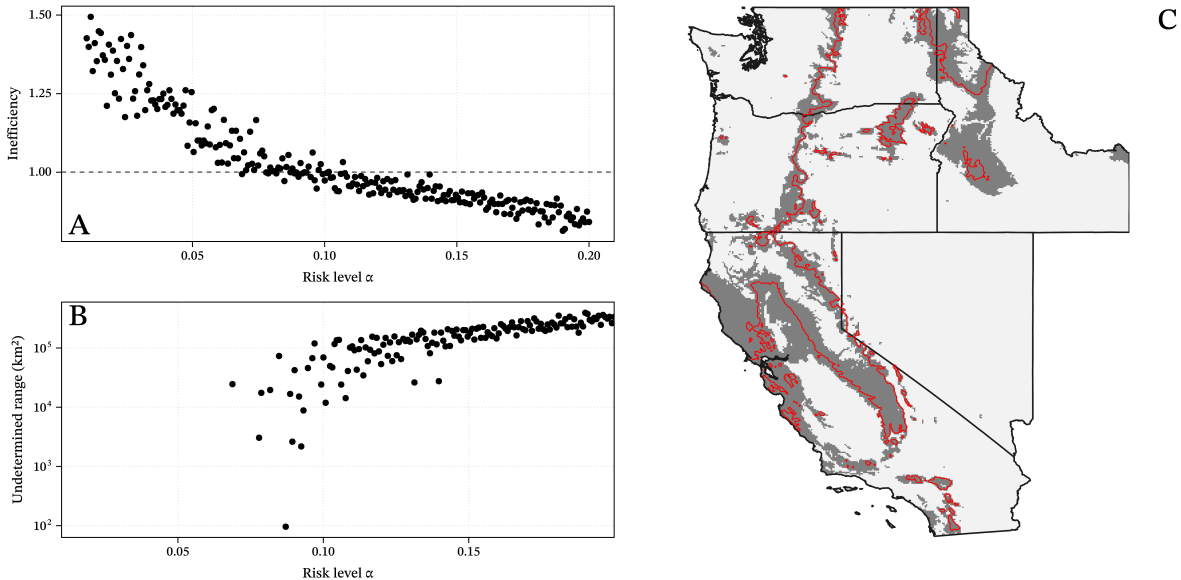
392 *Identification of undetermined areas*

393 In Figure 3B, we see that there is a risk level above which the total predicted range starts to get
394 lower than the range predicted by the SDM. We can explain this behavior through the lens of the
395 number of undetermined predictions, *i.e.* the number of inputs for which the CP model returns
396 $C = \emptyset$.

397 In fig. 4A, we see that above $\alpha \approx 0.1$, the inefficiency of the classifier starts to fall under 1 - this
398 indicates that *on average*, the model is returning fewer than one output for each prediction. In a
399 sense, this creates an upper limit to the risk we can accept: the model trained on this dataset does
400 not support conformal prediction for larger risk levels. In fig. 4B, we see that this change of
401 behavior in the model is indeed resulting in an increase in the range for which the model makes
402 no prediction, which gets larger when the risk level is too high. The spatial distribution of
403 undetermined areas is shown in fig. 4C for $\alpha = 0.2$: these areas are concentrated around the range
404 limit as identified by the SDM. This suggests that using a risk level that is too high would result to
405 no conformal predictions being made for the areas where our need to accurately quantify
406 uncertainty are the most important, and calls for a cautious investigation of the appropriate risk
407 level.

408 *Model explanation*

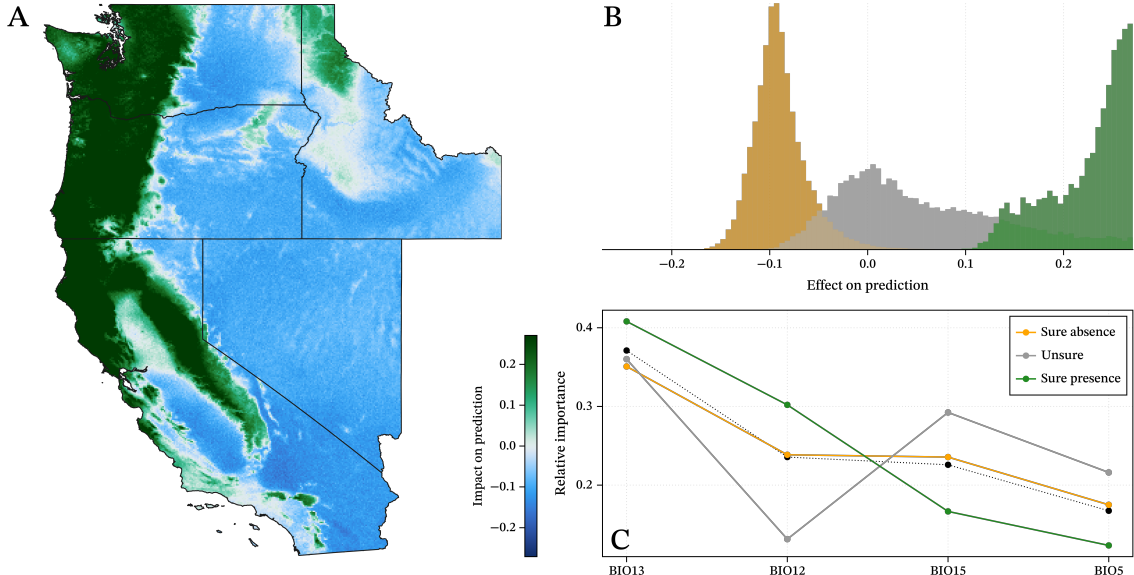
409 In this section, I perform an analysis of Shapley values of the conformal predictor, in order to (i)
410 assess the importance of variables and (ii) provide explainable results about the relationships
411 between predictors and response. I rely on the common Monte-Carlo approximation of Shapley



412 Figure 4: Inefficiency (average number of classes in the credible set) for various levels of α (A); above $\alpha \approx$
 413 0.1, the conformal prediction starts returning empty credible sets. This results in an increase in the spatial
 414 area for which no prediction can be made (B). For $\alpha = 0.2$, these areas are distributed around the limit of
 415 the predicted range, showing that the areas in which uncertainty quantification are most important cannot
 416 be predicted.

417 values (Roth 1988, Touati et al. 2021). Monte-Carlo Shapley values represent, for each prediction,
 418 how much the i th variable contributed to moving the prediction away from the average
 419 prediction. The Shapley value associated to variable i is $\varphi_i \in [-1, 1]$, which measures how much
 420 this variable modified the *average* prediction for this class. Shapley values have a number of
 421 desirable properties regarding the explanation of prediction of responses for environmental
 422 studies (Wadoux et al. 2023), including their additivity: for any given prediction, $p = \hat{p} +$
 423 $\sum_i^{\text{variables}} \varphi_i$. Because of this additive property, the importance of variables across many
 424 predictions is usually measured as the average of $|\varphi|$, where both positive (the class is more
 425 likely) and negative (the class is less likely) are counted. This measure of variable importance
 426 represents the relative impact that each variable had on the process of moving all predictions
 427 away from the average prediction and towards its actual value. Because Shapley values are both
 428 additive and independent, they can be measured and aggregated for any arbitrary stratification of
 429 the data (which allows reporting them conditional on the uncertainty status of the prediction).

430 As the predictions of the conformal model can be split by whether they are certain or uncertain,
 431 they offer a unique opportunity to delve into the mechanisms that *generate* this uncertainty.
 432 Namely, if the relative importance of variables is different across these classes of predictions, this



433 Figure 5: Overview of the effect of the most important predictor (A); areas with high values indicate that
 434 the value of BIO13 at this location make the presence of the species more likely. These values are associated
 435 to different prediction certainties (B), with predictions within the unsure range being centered around 0
 436 (i.e. not moving the needle on the average prediction one way or another). Nevertheless, the contribution of
 437 the variables in different uncertainty categories are different (C), suggesting that Shapley values can help
 438 create explanations of where uncertainty originates.

439 is strongly suggestive of the fact that there are certain environmental conditions (represented by
 440 combination of values for each variables) that create or reduce uncertainty. Furthermore, because
 441 we can split the certain predictions into a presence and absence class, this is a unique opportunity
 442 to investigate whether the factors leading to a species being present or absent are the same. An
 443 example of the spatial contribution of a variable is given in Figure 5A.

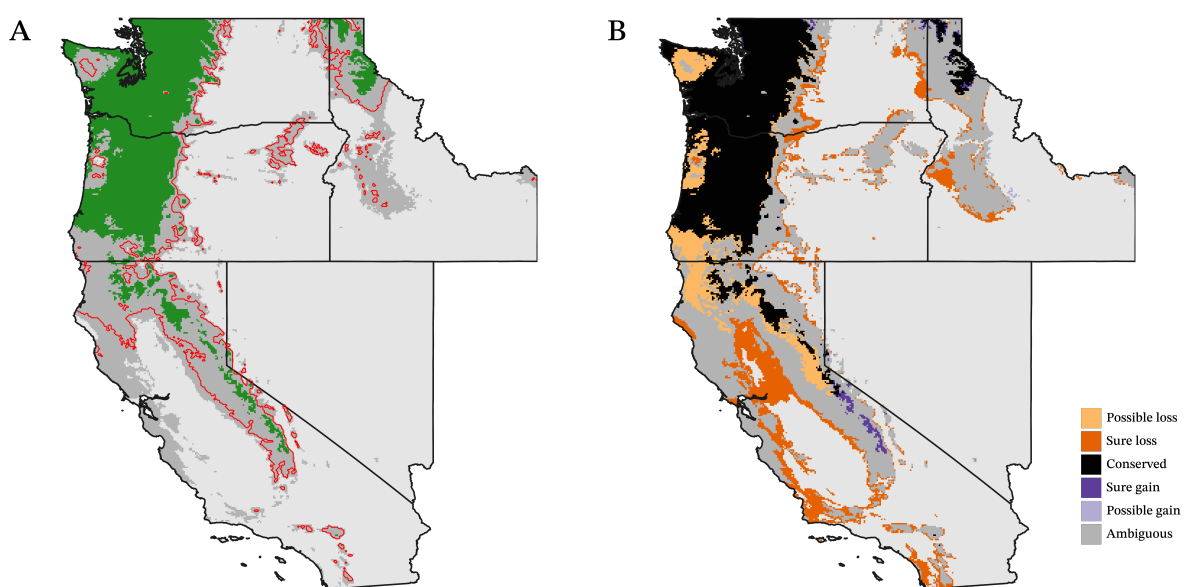
444 We find that, for the most important variable (*i.e.* the one with the largest $\sum|\varphi|$), the contribution
 445 of this variable tracks the status of the prediction: it tends to be negative when the absence is
 446 certain, positive when the presence is certain, and around zero when the prediction is unsure
 447 (fig. 5B). This is a fairly remarkable result, in that it ties Shapley values (a tool to help with ML
 448 models interpretation) to CP (a technique to accurately convey uncertainty). In Figure 5C, I
 449 present the relative contribution of all selected variables split by the status of the prediction; this
 450 reveals that the Shapley values for sure presences and unsure areas are distributed in different
 451 ways. Notably, BIO15 is far more important in areas of high model uncertainty than in areas of
 452 either sure presences or absences. This suggests that the division of the prediction according to
 453 CP status can provide information about which sets of environmental conditions are driving the

454 uncertainty, thereby providing useful information to guide future sampling or model
455 interpretation.

456 *Conformal prediction and climate-induced range shifts*

457 In a recent contribution, Smith & Levine (2025) suggest that because of issues around the use of
458 thresholds, projections of SDMs under climate change scenarios may benefit from a more
459 continuous perspective. In this section, I present a comparison of the conformal prediction of the
460 range under a climate change scenario (SSP370. 2081-2100), to illustrate how the future
461 conformal range can convey information about the certainty of some types of range shift. These
462 results are presented in Figure 6.

463 Based on the comparison between the baseline (fig. 2A) and projected (fig. 6A) ranges, we can
464 establish a series of transitions and their interpretations as range change scenarios, which are
465 presented in fig. 6B. Areas that are certain both now and in the future, $\{+\} \rightarrow \{+\}$, can safely be
466 assumed to be conserved. Areas that where unsure and become surely negative, $\{+,-\} \rightarrow \{-\}$ are
467 *possible losses*, as they may have been presences in the baseline data, but are considered lost in
468 the future. The reverse scenario, $\{+,-\} \rightarrow \{+\}$, corresponds to *possible gains*. Sure losses of range



469 Figure 6: Overview of the conformal prediction of the range for the future climate data, equivalent to
470 fig. 2A (panel A). Spatial distribution of areas where loss and gain are expected to be possible v. certain, as
471 explained in main text (B).

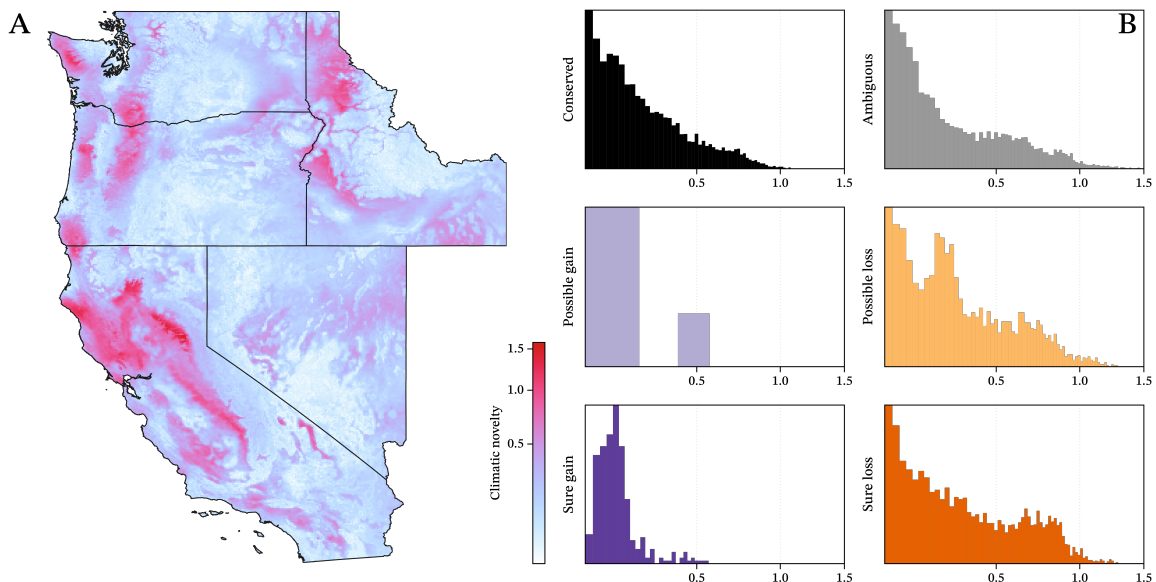
472 correspond to the transition $\{+\} \rightarrow \{-\}$, and sure gains of range correspond to $\{-\} \rightarrow \{+\}$. Other
473 situations are considered ambiguous.

474 By applying these rules on the predicted changes in presence/absence status, we can identify
475 large areas that are confidently loss towards the Southern edge of the species's range, with very
476 limited areas of either possible or sure gain, strongly suggesting that this species would undergo
477 range contraction. Note that the area corresponding to ambiguous transitions is relatively large,
478 which provides a good understanding of the possible variation to be expected under this climate
479 change scenario.

480 *Conformal prediction and climatic novelty*

481 Zurell et al. (2012) highlight the importance of fully considering uncertainty when transferring
482 the model to novel climate data: there is a chance that the future climate conditions will not have
483 occurred in the training dataset, and therefore our confidence in the model outcome should be
484 lowered. This covariate shift is well documented to decrease the performance of models
485 (Mesgaran et al. 2014), and CP offers an opportunity to shine a different light on this
486 phenomenon.

487 This task is particularly crucial given that entirely novel climatic conditions are likely to become
488 the norm (Mahony et al. 2017), which in turn will drive the emergence of a novel biosphere
489 globally (Kerr et al. 2025, Ordonez et al. 2024). In this section, I compare the results of
490 conformation prediction to measures of climatic novelty, by partitioning the climate novelty
491 according to the type of range shifts from fig. 6B. The study area shows higher novelty in parts of
492 the range that are currently predicted to be habitable by the species; nevertheless, this does not
493 translate to an association between types of prediction transition and the distribution of novelty
494 within the regions undergoing this transition. In other words, the projected uncertainty under
495 conformal prediction contributes different information when compared to measures of climatic
496 novelty; specifically, it conveys the uncertainty tied to the model itself.



497 Figure 7: Climate novelty measured as Euclidean distance to the closest contemporary analogue (A); note
 498 that the scale is square-root transformed, as most areas show low novelty. Distribution of novelty values
 499 split by the expected transition in occupancy (B); colors are as in fig. 6B.

500 Conclusion

501 Conformal prediction, like most SDM methods, is not quite delivering a true estimate of the
 502 probability of presence (Phillips & Elith 2013). Nevertheless, it brings valuable information, in the
 503 form of a quantified measure of whether a prediction comes with uncertainty (are both presence
 504 and absence in the credible set?) in a way that is directly comparable with the non-conformal
 505 prediction. “Class overlap”, where both presences and absences are observed under the same
 506 values of the predictions, decreases the predictive performance of models (Valavi et al. 2021) —
 507 CP is naturally suited at handling this, by assigning the area where overlap occurs to uncertain
 508 predictions.

509 Transparent communication of uncertainty, meaning that it is both spatially explicit, quantified,
 510 and expressed under a risk set by the user, is important: we do not expect a fully trained model to
 511 always be certain, as some areas are genuinely more difficult to predict. For example, small
 512 organisms are more inherently stochastic (Soininen et al. 2013) any form of stochastic event will
 513 drive species distribution even when there is strong environmental signal (Mohd et al. 2016) these
 514 stochastic events can even manifest in areas that are close to the species’ environmental optimum

515 (Dallas et al. 2020). For these reasons, CP can produce interpretable estimates of uncertainty in
516 species distribution models, and does not require the adoption of additional modeling tools or
517 paradigms as it functions on an already trained model.

518 CP contributes to dispel what Messeri & Crockett (2024) called the “illusion of understanding”,
519 which is often associated with ML models: it generates an understanding of the uncertainty from
520 observations of a pre-trained model, and expresses this uncertainty both in absolute (is the
521 “presence” event in the credible set?) and relative (is the point estimate of the score for presence
522 larger than for absence?) terms. Because this technique is computationally efficient and works on
523 pre-trained models, it opens up the opportunity for more systematic uncertainty quantification
524 (Zurell et al. 2020) in SDMs. CP, in short, can deliver the “maps of ignorance” that Rocchini et al.
525 (2011) argued for: how difficult is it to make a prediction for the range at a given risk level is, in
526 and of itself, an important information to frame the reliability of the results. Finally, CP can
527 provide guidance on the feedback loop between SDM training and field validation (Johnson et al.
528 2023) — areas where the range is certain are a much lower priority for sampling.

529 Bibliography

- 530 Aldous DJ. 1985. Exchangeability and related topics. In *Lecture Notes in Mathematics*, pp. 1–198.
531 Berlin, Heidelberg: Springer Berlin Heidelberg
- 532 Allouche O, Tsoar A, Kadmon R. 2006. Assessing the accuracy of species distribution models:
533 prevalence, kappa and the true skill statistic (TSS). *The journal of applied ecology*. 43(6):1223–
534 32
- 535 Angelopoulos AN, Bates S. 2023. *Conformal Prediction: A Gentle Introduction*. Hanover, MD: now
- 536 Balayla J. 2020. Prevalence threshold (ϕ_e) and the geometry of screening curves. *PloS one*.
537 15(10):e240215

- 538 Barbet-Massin M, Jiguet F, Albert CH, Thuiller W. 2012. Selecting pseudo-absences for species
539 distribution models: how, where and how many?: How to use pseudo-absences in niche
540 modelling?. *Methods in ecology and evolution*. 3(2):327–38
- 541 Beale CM, Lennon JJ. 2012. Incorporating uncertainty in predictive species distribution
542 modelling. *Philosophical transactions of the Royal Society of London. Series B, Biological
543 sciences*. 367(1586):247–58
- 544 Beery S, Cole E, Parker J, Perona P, Winner K. 2021. Species Distribution Modeling for machine
545 learning practitioners: A review. *arXiv [cs.LG]*
- 546 Benkendorf DJ, Schwartz SD, Cutler DR, Hawkins CP. 2023. Correcting for the effects of class
547 imbalance improves the performance of machine-learning based species distribution models.
548 *Ecological modelling*. 483(110414):110414
- 549 Bylander T. 2002. Estimating Generalization Error on Two-Class Datasets Using Out-of-Bag
550 Estimates. *Machine learning*. 48(1/3):287–97
- 551 Carlson CJ. 2020. embarcadero: Species distribution modelling with Bayesian additive regression
552 trees in r. *Methods in ecology and evolution*. 11(7):850–58
- 553 Chen X, Dimitrov NB, Meyers LA. 2019. Uncertainty analysis of species distribution models. *PloS
554 one*. 14(5):e214190
- 555 Chicco D, Jurman G. 2023. The Matthews correlation coefficient (MCC) should replace the ROC
556 AUC as the standard metric for assessing binary classification. *BioData mining*. 16(1):4
- 557 Dallas TA, Santini L, Decker R, Hastings A. 2020. Weighing the Evidence for the Abundant-
558 Center Hypothesis. *Biodiversity informatics*. 15(3):81–91
- 559 Davies SC, Thompson PL, Gomez C, Nephin J, Knudby A, et al. 2023. Addressing uncertainty
560 when projecting marine species' distributions under climate change. *Ecography*. 2023(11):
- 561 Drake JM. 2014. Ensemble algorithms for ecological niche modeling from presence-background
562 and presence-only data. *Ecosphere (Washington, D.C.)*. 5(6):1–16

- 563 Elith J. 2019. Species Distribution Modeling
- 564 Fannjiang C, Bates S, Angelopoulos AN, Listgarten J, Jordan MI. 2022. Conformal prediction
565 under feedback covariate shift for biomolecular design. *Proceedings of the National Academy
566 of Sciences of the United States of America*. 119(43):e2204569119
- 567 Feng X, Park DS, Walker C, Peterson AT, Merow C, Papeş M. 2019. A checklist for maximizing
568 reproducibility of ecological niche models. *Nature ecology & evolution*. 3(10):1382–95
- 569 Fick SE, Hijmans RJ. 2017. WorldClim 2: new 1-km spatial resolution climate surfaces for global
570 land areas: NEW CLIMATE SURFACES FOR GLOBAL LAND AREAS. *International journal
571 of climatology: a journal of the Royal Meteorological Society*. 37(12):4302–15
- 572 Fitzpatrick MC, Blois JL, Williams JW, Nieto-Lugilde D, Maguire KC, Lorenz DJ. 2018. How will
573 climate novelty influence ecological forecasts? Using the Quaternary to assess future
574 reliability. *Global Change Biology*. 24(8):3575–86
- 575 Fontana M, Zeni G, Vantini S. 2020. Conformal Prediction: A unified review of theory and new
576 challenges. *arXiv [cs.LG]*
- 577 Foxon F. 2024. Bigfoot: If it's there, could it be a bear?. *Journal of zoology (London, England: 1987)*
- 578 Franklin J. 2023. Species distribution modelling supports the study of past, present and future
579 biogeographies. *Journal of biogeography*. 50(9):1533–45
- 580 Gammerman A, Vovk V, Vapnik V. 1998. Learning by transduction. *Proceedings of the Fourteenth
581 Conference on Uncertainty in Artificial Intelligence*. 148–55. San Francisco, CA, USA: Morgan
582 Kaufmann Publishers Inc.
- 583 Janitza S, Hornung R. 2018. On the overestimation of random forest's out-of-bag error. *PloS one*.
584 13(8):e201904
- 585 Johnson S, Molano-Flores B, Zaya D. 2023. Field validation as a tool for mitigating uncertainty in
586 species distribution modeling for conservation planning. *Conservation science and practice*.
587 5(8):e12978

- 588 Kerr MR, Ordonez A, Riede F, Atkinson J, Pearce EA, et al. 2025. Widespread ecological novelty
589 across the terrestrial biosphere. *Nature ecology & evolution*. 1–10
- 590 Lei J, Wasserman L. 2013. Distribution-free Prediction Bands for Non-parametric Regression.
591 *Journal of the Royal Statistical Society. Series B, Statistical methodology*. 76(1):71–96
- 592 Liu C, Newell G, White M. 2016. On the selection of thresholds for predicting species occurrence
593 with presence-only data. *Ecology and evolution*. 6(1):337–48
- 594 Liu C, White M, Newell G. 2013. Selecting thresholds for the prediction of species occurrence
595 with presence-only data. *Journal of biogeography*. 40(4):778–89
- 596 Lozier JD, Aniello P, Hickerson MJ. 2009. Predicting the distribution of Sasquatch in western
597 North America: anything goes with ecological niche modelling. *Journal of biogeography*.
598 36(9):1623–27
- 599 Mahony CR, Cannon AJ, Wang T, Aitken SN. 2017. A closer look at novel climates: new methods
600 and insights at continental to landscape scales. *Global change biology*. 23(9):3934–55
- 601 Mesgarian MB, Cousens RD, Webber BL. 2014. Here be dragons: a tool for quantifying novelty due
602 to covariate range and correlation change when projecting species distribution models.
603 *Diversity & distributions*. 20(10):1147–59
- 604 Messeri L, Crockett MJ. 2024. Artificial intelligence and illusions of understanding in scientific
605 research. *Nature*. 627(8002):49–58
- 606 Mohd MH, Murray R, Plank MJ, Godsoe W. 2016. Effects of dispersal and stochasticity on the
607 presence–absence of multiple species. *Ecological modelling*. 342:49–59
- 608 Neyman J. 1937. Outline of a theory of statistical estimation based on the classical theory of
609 probability. *Philosophical transactions of the Royal Society of London*. 236(767):333–80
- 610 Oliveira RI, Orenstein P, Ramos T, Romano JV. 2024. Split conformal prediction and non-
611 exchangeable data. *Journal of machine learning research: JMLR*. 25(225):1–38

- 612 Ordonez A, Riede F, Normand S, Svenning J-C. 2024. Towards a novel biosphere in 2300: rapid
613 and extensive global and biome-wide climatic novelty in the Anthropocene. *Philosophical*
614 *transactions of the Royal Society of London. Series B, Biological sciences.* 379(1902):
615 Parker EJ, Weiskopf SR, Oliver RY, Rubenstein MA, Jetz W. 2024. Insufficient and biased
616 representation of species geographic responses to climate change. *Global change biology.*
617 30(7):e17408
- 618 Petitpierre B, Broennimann O, Kueffer C, Daehler C, Guisan A. 2016. Selecting predictors to
619 maximize the transferability of species distribution models: lessons from cross-continental
620 plant invasions. *Global ecology and biogeography: a journal of macroecology.* 26(3):275–87
- 621 Petropoulos F, Hyndman RJ, Bergmeir C. 2018. Exploring the sources of uncertainty: Why does
622 bagging for time series forecasting work?. *European journal of operational research.*
623 268(2):545–54
- 624 Phillips SJ, Elith J. 2013. On estimating probability of presence from use-availability or presence-
625 background data. *Ecology.* 94(6):1409–19
- 626 Poisot T, Bussières-Fournel A, Dansereau G, Catchen MD. 2025. A Julia toolkit for species
627 distribution data. *EcoEvoRxiv*
- 628 Prescott VA, Marte J, Keller RP. 2025. Performance of alternative methods for generating species
629 distribution models for invasive species in the Laurentian Great Lakes. *Fisheries.* vuaf12
- 630 Pěknicová J, Berchová-Bímová K. 2016. Application of species distribution models for protected
631 areas threatened by invasive plants. *Journal for nature conservation.* 34:1–7
- 632 Rocchini D, Hortal J, Lengyel S, Lobo JM, Jiménez-Valverde A, et al. 2011. Accounting for
633 uncertainty when mapping species distributions: The need for maps of ignorance. *Progress in*
634 *physical geography.* 35(2):211–26
- 635 Romano Y, Patterson E, Candès E. 2019. Conformalized Quantile Regression. *Neural Information*
636 *Processing Systems.* 32:3538–48

- 637 Romano Y, Sesia M, Candès EJ. 2020. Classification with valid and adaptive coverage. *Proceedings*
638 *of the 34th International Conference on Neural Information Processing Systems*. 3581–91. Red
639 Hook, NY, USA: Curran Associates Inc.
- 640 Roth AE. 1988. Introduction to the Shapley value. In , pp. 1–28. Cambridge University Press
- 641 Sadinle M, Lei J, Wasserman L. 2018. Least Ambiguous Set-Valued Classifiers With Bounded
642 Error Levels. *Journal of the American Statistical Association*. 114(525):223–34
- 643 Shafer G, Vovk V. 2007. A tutorial on conformal prediction. *Journal of machine learning research:*
644 *JMLR*. (12):371–421
- 645 Smith JR, Levine JM. 2025. Linking relative suitability to probability of occurrence in presence-
646 only species distribution models: Implications for global change projections. *Methods in*
647 *ecology and evolution*
- 648 Soininen J, Korhonen JJ, Luoto M. 2013. Stochastic species distributions are driven by organism
649 size. *Ecology*. 94(3):660–70
- 650 Soley-Guardia M, Alvarado-Serrano DF, Anderson RP. 2024. Top ten hazards to avoid when
651 modeling species distributions: a didactic guide of assumptions, problems, and
652 recommendations. *Ecography*. 2024(4):
- 653 Szeghalmy S, Fazekas A. 2023. A comparative study of the use of stratified cross-validation and
654 distribution-balanced stratified cross-validation in imbalanced learning. *Sensors (Basel,*
655 *Switzerland)*. 23(4):
- 656 Thuiller W, Guéguen M, Renaud J, Karger DN, Zimmermann NE. 2019. Uncertainty in ensembles
657 of global biodiversity scenarios. *Nature communications*. 10(1):1446
- 658 Tibshirani RJ, Barber RF, Candes EJ, Ramdas A. 2019. Conformal Prediction Under Covariate
659 Shift. *arXiv [stat.ME]*
- 660 Touati S, Radjef MS, Sais L. 2021. A Bayesian Monte Carlo method for computing the Shapley
661 value: Application to weighted voting and bin packing games. *Computers & operations*
662 *research*. 125:105094

- 663 Valavi R, Elith J, Lahoz-Monfort JJ, Guillera-Arroita G. 2021. Modelling species presence-only
664 data with random forests. *Ecography*. 44(12):1731–42
- 665 Vovk V, Nouretdinov I, Manokhin V, Gammerman A. 2018. Cross-conformal predictive
666 distributions. *Proceedings of the Seventh Workshop on Conformal and Probabilistic Prediction
667 and Applications*. 91:37–51
- 668 Wadoux AMJ-C, Saby NPA, Martin MP. 2023. Shapley values reveal the drivers of soil organic
669 carbon stock prediction. *SOIL*. 9(1):21–38
- 670 Zurell D, Elith J, Schröder B. 2012. Predicting to new environments: tools for visualizing model
671 behaviour and impacts on mapped distributions. *Diversity & distributions*. 18(6):628–34
- 672 Zurell D, Franklin J, König C, Bouchet PJ, Dormann CF, et al. 2020. A standard protocol for
673 reporting species distribution models. *Ecography*. 43(9):1261–77